Hindawi
Journal of Food Quality
Volume 2019, Article ID 2623404, 13 pages
https://doi.org/10.1155/2019/2623404

Research Article

Thermal Diffusivity, Moisture Diffusivity, and Color Change of *Codonopsis javanica* with the Support of the Ultrasound for Drying

Xuan-Quang Nguyen,[1] **Anh-Duc Le**,[2] **Ngoc-Phuong Nguyen**,[1] **and Hay Nguyen**[2]

[1]*Faculty of Mechanical Engineering, Ho Chi Minh City University of Technology and Education, Ho Chi Minh City, Vietnam*
[2]*Faculty of Engineering and Technology, Nong Lam University, Ho Chi Minh City, Vietnam*

Correspondence should be addressed to Hay Nguyen; ng.hay@hcmuaf.edu.vn

Received 25 July 2019; Revised 23 September 2019; Accepted 8 October 2019; Published 3 November 2019

Academic Editor: Vera Lavelli

Copyright © 2019 Xuan-Quang Nguyen et al. This is an open access article distributed under the Creative Commons Attribution License, which permits unrestricted use, distribution, and reproduction in any medium, provided the original work is properly cited.

In this study, drying kinetics, including thermal and moisture, of *Codonopsis javanica* with the support of ultrasonic technology in the drying process were investigated. Experimental processes were carried out at drying air temperatures of 40°C, 45°C, and 50°C with and without ultrasound at a frequency of 20 kHz and three levels of intensity: 1.3 kW/m^2, 1.8 kW/m^2, and 2.2 kW/m^2. Based on theoretical calculations, experimental data, and the particle swarm optimization (PSO) algorithm, the coefficient of thermal diffusion was determined in the range of $1.01–1.36 \times 10^{-7}$ m^2/s, and the coefficient of moisture diffusion is in the range of $3.2–6.7 \times 10^{-10}$ m^2/s. In addition, the color parameters (L^*, a^*, and b^*) of the drying materials were also considered. Results showed the overall color differences (ΔE) of dried products change in the range of 8.0–12.9 compared with the fresh ones. In this work, the multiple boundary conditions were considered to determine the moisture and thermal diffusion coefficients; the results obtained prove that the quality of dried products in terms of color change is also improved.

1. Introduction

Codonopsis javanica is an agricultural product of high economic value in Vietnam, used for food and medicine. So, its moisture content reduction is necessary for preservation. *C. javanica* is a heat-sensitive material; therefore, drying air temperature and drying time affect the nutrient composition, herbal medicine, and product color.

Ultrasound-assisted drying is a high-energy mechanical wave (its frequencies range between 18 kHz and 100 kHz [1, 2]) and considered a hybrid drying technique to reduce drying time, save energy, and maintain the nutrient composition of the products [3]. The energy of ultrasound reduces the internal and external resistances to moisture transfer in the material. In addition, microstreaming at the surface of the drying material, caused by ultrasound, decreases the diffusion boundary layer and enhances drying kinetics and diffusivity [4]. This affects the drying kinetics of the material whose characteristic quantity is the effective diffusion coefficient (D_e). With no external resistance factors, the effective diffusion coefficient was calculated from the diffusion equation based on Fick's second law [4]. Assuming that deformation of objects during drying is negligible, using the initial conditions and the reasonable constraints, Crank [5] determined the solutions of the diffusion equations in different geometrical conditions. Applying Fick's second law and Crank's results, the researchers determined the moisture diffusion coefficients of orange peel [6], salted cod [7], honeysuckle [8], and apple slabs [9]. Considering the external resistance factors, the conditions of moisture exchange at the surface of the drying materials and drying air are investigated, and the effective diffusion coefficient (D_e) and moisture transfer coefficients (h_m) at the surface would be determined simultaneously. Previous studies [6, 10–12] accomplished this by combining theoretical calculations, experimental data, and the optimal algorithm with the appropriate objective function, to find parameters of orange, apple, strawberry, and passion fruit

peel. Rodríguez et al. suggested a heat and mass transfer model and solved the optimization problem to obtain the thermal and mass transfer coefficients for thyme leaves [13]. The differences of the moisture content of materials between the experimental data and theoretical calculations when considering external resistance factors are less than the differences of those when no external resistance factors apply [6, 12]. It can be seen that in order to reduce the error of the calculated and experimental moisture content in drying processes, with the support of ultrasound, one should consider the external resistance factors. In this paper, therefore, the well-known PSO algorithm is employed to determine the appropriate parameters related to the drying kinetics.

When Bantle et al. used ultrasound-assisted drying, the temperature in salt fish was higher than 5°C compared with drying without ultrasound [14, 15]. When drying was supported by ultrasound, the temperature at the surface of apples was higher from 1.0°C to 1.5°C [16]. Evidently, ultrasound-assisted drying affects not only moisture diffusion but also thermal diffusion in drying materials, heat, and moisture transfer between drying materials and drying air.

Musielak et al. published a review of research on ultrasound-assisted drying [1] influencing many scholars to perform testing on a variety of agricultural products and foods. These studies focus mostly on moisture diffusivity analysis of drying kinetics. We realized that studying *C. javanica* has not yet been done, and the study of moisture and thermal diffusion using the multiple parameters considered at the boundary conditions is still limited. In the present study, therefore, moisture and thermal diffusion coefficients were determined, and a comparison of color change of the products with ultrasound was performed.

2. Materials and Methods

2.1. Materials. Fresh four-year-old *C. javanica* samples were cultivated in Lam Dong province, Vietnam. Their average diameters were approximately 20–25 mm. After harvesting, they were stored in refrigerator conditions at 5°C. Before conducting the experiments, they were sliced to a thickness of 5 ± 0.5 mm. The initial temperature was 25–27°C, and the initial moisture content was 6.4–7.7 (kg W/kg DM (dry matter)). The moisture content of the samples was determined by using a moisture analyzer (DBS 60-3).

2.2. Drying Experiments and Procedures. The experiment system consisted of a heat pump dryer integrated with an ultrasonic transducer in the drying chamber (Figure 1(a)). The drying air was created by the dryer system with a temperature range of 28–50°C, relative humidity between 12–58%, and air velocity from 0.1 to 2.5 m/s. High-energy ultrasound was emitted from a transmitter, which was developed previously [17]; its frequency and intensity were 20 ± 0.73 kHz and in the range of 0–3.0 kW/m^2, respectively. The samples were weighed online with respect to time by an electronic weight scale (GX-200) with an accuracy of ±0.001 g. The temperature of the drying air and samples was measured by sensors (Fluke 5622-10-s) with an accuracy of ±0.09°C and 1 mm diameter. The system and material parameters were updated and stored automatically in a computer.

2.2.1. Experimental Procedures to Determine the Ultrasonic Absorption Coefficient of C. javanica. Material slices with 5 mm thickness and 25 mm diameter were placed on the tray at the distance of 8.5 mm to the emitter. Two temperature sensors were used for each slice (a sensor in the center (point B), the other was close to the surface inside the material (point A), Figure 1(b)). To determine the temperature differences in the drying material with and without ultrasound, (i) the material was placed in the drying chamber (Figure 1(a)); the temperature in the chamber was maintained at 40°C and the ultrasound was emitted continuously. (ii) After approximately 60 minutes, when the system reached a steady state, the ultrasound was turned off for 10 minutes; thereafter, the ultrasound was emitted every 5 minutes, and the data were recorded at the beginning and the end of the cycle. The experiments were repeated three times per sample.

2.2.2. Experimental Procedures to Determine Drying Kinetics of C. javanica. Each batch of drying consisted of 100 g materials. The original colors of fresh materials were measured before putting them on the sample tray. Twelve cases (cases 1–12) were investigated corresponding to 12 different experimental conditions, where temperatures were 40°C, 45°C, and 50°C with an accuracy of ±0.5°C; the air velocity was fixed at 0.5 m/s, with and without the support of ultrasound at three levels of intensity: $I_{u1} = 1.3$ kW/m^2, $I_{u2} = 1.8$ kW/m^2, and $I_{u3} = 2.2$ kW/m^2. The experiment was terminated when the moisture content of the material reached an equilibrium state. Each test case was repeated three times; the final data were averaged of the three repetitions. The weight and temperature at points A and B of the dried samples were updated and stored automatically in a computer at a sampling time of 10 minutes. To minimize the error in each sample, the ultrasonic sound was stopped, and the air was not blown into the drying chamber for 10 seconds.

2.3. Modeling. The thickness of the material was low compared with its diameter; thus, it is reasonable to assume that heat and moisture transfer is only considered in the thickness direction (z-axis). The mathematical model used to calculate the drying process was the one-dimensional Fourier's law of heat, which is described by the following equation:

$$\frac{\partial t}{\partial \tau} = \alpha_t \frac{\partial^2 t}{\partial z^2}. \quad (1)$$

Moisture transfer in the drying material is also described by the following diffusion equation [6, 7, 11, 12]:

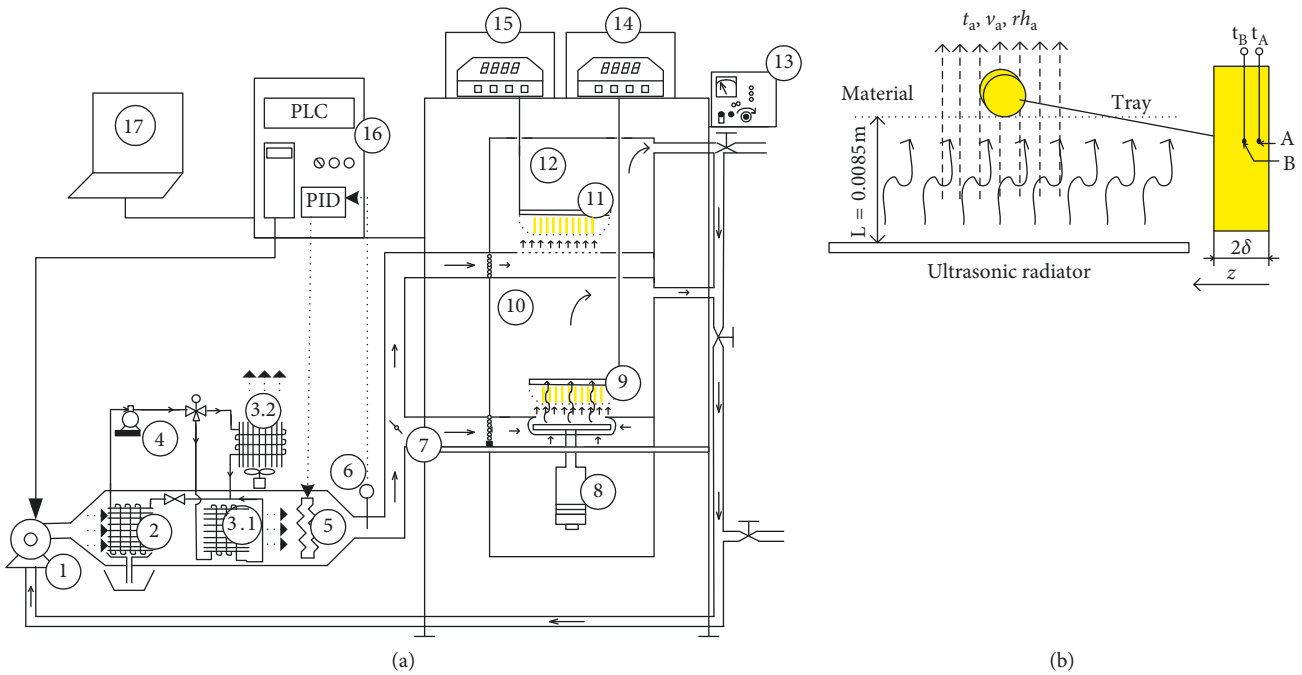


FIGURE 1: The experiment setup of the drying process. (a) The drying system using a heat pump method and ultrasound. (b) The position of the material in the drying chamber and its two points of temperature measurement (A and B). (1) Drying fan; (2) evaporator; (3.1), (3.2) condenser; (4) compressor; (5) auxiliary air heater; (6) temperature and humidity sensors; (7) valve; (8) ultrasonic transducer; (9), (11) trays for samples; (10) drying chamber with ultrasound; (12) drying chamber without ultrasound; (13) high-power ultrasonic generator; (14), (15) electronic weight scale; (16) unit controller; (17) computer.

$$\frac{\partial M}{\partial \tau} = D_e \frac{\partial^2 M}{\partial z^2}, \tag{2}$$

where τ: time (s); z, coordinate (m); M: moisture content of materials (kg W/kg DM); t: temperature (°C); a_t: thermal diffusivity (m^2/s); and D_e: effective moisture diffusivity (m^2/s).

The initial conditions of temperature and moisture ($\tau = 0$) of the drying material were uniform (equation (3)); heat and moisture transfer at both sides of the material was identical (geometric symmetry) (equation (4)):

$$\tau = 0; t(z,0) = t_0,\ M(z,0) = M_0, \tag{3}$$

$$z = 0, \tau \neq 0;\ \frac{\partial t(0,\tau)}{\partial z} = 0,\ \frac{\partial M(0,\tau)}{\partial z} = 0. \tag{4}$$

Assuming that the heat flux absorbed into the material included the convective heat transfer from the drying air and the difference between the absorption heat by the ultrasound and the evaporation heat. The boundary conditions of the convective heat transfer at the surface of the drying material with the support of ultrasound were determined by the following equation:

$$z = \delta, \tau > 0; -k_p \frac{\partial t(\delta,\tau)}{\partial z} = h_t\left[t_a - t(\delta,\tau)\right] + \mu_u I_u - D_e \rho_s h_{fg} \frac{\partial M(\delta,\tau)}{\partial z}. \tag{5}$$

To consider the effect of ultrasound on convective moisture transfer at the surface of the drying material, the boundary conditions (equation (6)) were used to solve the equations of moisture transfer [6, 11, 12]:

$$z = \delta, \tau > 0; -D_e \rho_s \frac{\partial M(\delta,\tau)}{\partial z} = h_m\left[\varphi_e(\delta,t) - \varphi_a\right], \tag{6}$$

where h_m: convective moisture transfer coefficient (kg/m^2s); h_{fg}: latent heat of vaporization (J/kg); φ_e: water activity (a_w) at the surface of the drying material (0–1); φ_a: moisture of the drying air (0–1); h_t: convective heat transfer coefficient at the surface of the drying material (W/m^2 K); t_a: temperature of the drying air (°C); ρ_s and ρ_p: density of the dry solid and the material (kg/m^3); k_p: thermal conductivity of the material (W/m K); μ_u: ultrasonic absorption coefficient; and I_u: ultrasound intensity (kW/m^2).

2.4. Determination of Moisture Content. The moisture content of the material (dry basis) was determined by the following equation:

$$M = \frac{m_t - m_s}{m_s}, \tag{7}$$

where M: moisture content; m_t: weight of the material; and m_s: weight of the dry solid.

2.5. Determination of Ultrasonic Absorption Coefficient of Material. When the ultrasound propagates a material, part of its energy is absorbed by the material and converted into thermal energy, increasing the temperature of the material [16]. To evaluate the absorbing capability of the material for

ultrasonic energy, the parameter μ_u is presented [16]. In this study, assuming that the energy absorbed by the material from the ultrasound is converted into thermal energy, we applied the law of energy conservation to derive the parameter μ_u in the following equation:

$$\mu_u = \frac{2\delta\rho_p c_p \Delta t_{av}}{\Delta\tau I_u}, \tag{8}$$

where Δt_{av} is the average increased temperature in the period of time $\Delta\tau$ which is calculated in the following equation:

$$\Delta t_{av} = \frac{\Delta t_A + \Delta t_B}{2}, \tag{9}$$

where Δt_A and Δt_B are the temperature differences in the drying material with and without ultrasound at points A and B, respectively.

It can be considered that the components of *C. javanica* are similar to Korean Ginseng. Hence, heat capacity and density of this material can be determined from Korean Ginseng, which are $c_p = 2605.492$ J/kg K and $\rho_p = 1361.6$ kg/m^3, respectively [18].

2.6. Determination of Equilibrium Moisture Content of Material. At certain conditions of temperature and water activity (a_w), after a period of time, the moisture in the material reaches an equilibrium state (M_e) (a necessary parameter to calculate the diffusion coefficient). The static gravimetric method using a saturated salt solution was applied to determine the equilibrium moisture content in *C. javanica* samples. The experiments were carried out at three levels of temperature 30°C, 45°C, and 50°C and 21 levels of water activity from 0.111 to 0.923 created by seven types of salts: lithium chloride, potassium fluoride, magnesium chloride, sodium bromide, potassium chloride, sodium chloride, and potassium nitrate [11, 19]. The mathematical models proposed by Henderson, Chung–Pfost, Halsey [19], and Oswin [18] were adopted to predict the equilibrium moisture content of *C. javanica*. The nonlinear regression method was used to obtain the parameters of the regression equations. The suitable model was chosen based on some criteria of coefficient of determination (R^2), root mean square error (RMSE), and mean relative percentage error (MRE).

2.7. Determination of Drying Kinetics. To study thermal and moisture diffusion of the materials, all parameters in equations (1) and (2) must be determined. The parameters with the physical thermal property, k_p, ρ_p, and ρ_s can be obtained from experiments. However, h_t and h_m values are difficult to determine for the effects of ultrasound and oscillation of gas molecules around the drying material with the properties being in flux. In addition, when considering the external resistance effect and support of ultrasound, more parameters are needed. In this study, theoretical calculations together with the experimental results and the particle swarm optimization (PSO) algorithm were utilized to determine necessary parameters including thermal diffusivity (α_t), effective moisture diffusivity (D_e), convective heat, and moisture transfer coefficients (h_t and h_m).

Heat and moisture transfer equations (equations (1) and (2)) were solved by the explicit finite difference approximation method with a number of nodes, with respect to thickness direction ($N = 15$). Equation (10) shows the size of a step distance; equation (11) shows the size of a step time:

$$\Delta z = \frac{2\delta}{N-1}, \tag{10}$$

$$\Delta\tau = \frac{0.4[2\delta/N-1]^2}{\alpha_t}. \tag{11}$$

The average moisture and temperature of the volume at the time (m) were determined by the following equations:

$$M_{av}^m = \frac{(\Delta z/2)M_1^m + \sum_{i=2}^{(N-3)/2}\Delta z M_i^m + (\Delta z/2)M_{(N-1)/2}^m}{(\Delta z/2)[N-1]}, \tag{12}$$

$$t_{av}^m = \frac{(\Delta z/2)t_1^m + \sum_{i=2}^{(N-3)/2}\Delta z t_i^m + (\Delta z/2)t_{(N-1)/2}^m}{(\Delta z/2)[N-1]}. \tag{13}$$

The search algorithm would determine the values of D_e, α_t, h_m, and h_t in the predefined constraints. Differential equations (1) and (2), which are subject to the initial and boundary conditions (equations (3)–(6)), were solved to determine the moisture and temperature profile in the material. The average moisture in the volume of the drying material (M_{av}) and the average temperature of the drying material (t_{av}) were determined as well (equations (12) and (13)). The objective function, equation (16), is defined as the differences between theoretical calculations and experimental data of moisture and temperature of the drying material. The algorithm would determine the values of D_e, α_t, h_m, and h_t and their constraints to minimize the objective function, equation (17). This algorithm is illustrated in Figure 2.

The PSO algorithm was used in this study as the search algorithm, its multi-objective optimization technique gives high-precision results for linear and nonlinear models [20]. Its concept is based on the behavior of looking for foods within a swarm [21]. Each particle has a position in the search space that represents a parameter value and a velocity vector used to update a new position. The particles start with random values in a predefined space and are modified to find the best variation. At each step, all particles are updated with the best two solution values: P_{best}, personal best position so far and G_{best}, global best position up to now. The position and velocity of each particle are accelerated toward the global best, and its own personal best based on the following equations [21]:

$$v_i(m+1) = \omega v_i(m+1) + c_1 w_1\left[x_{P_{best}} - x_i(m)\right] + c_2 w_2\left[x_{G_{best}} - x_i(m)\right], \tag{14}$$

$$x_i(m+1) = x_i(m) + v_i(m+1). \tag{15}$$

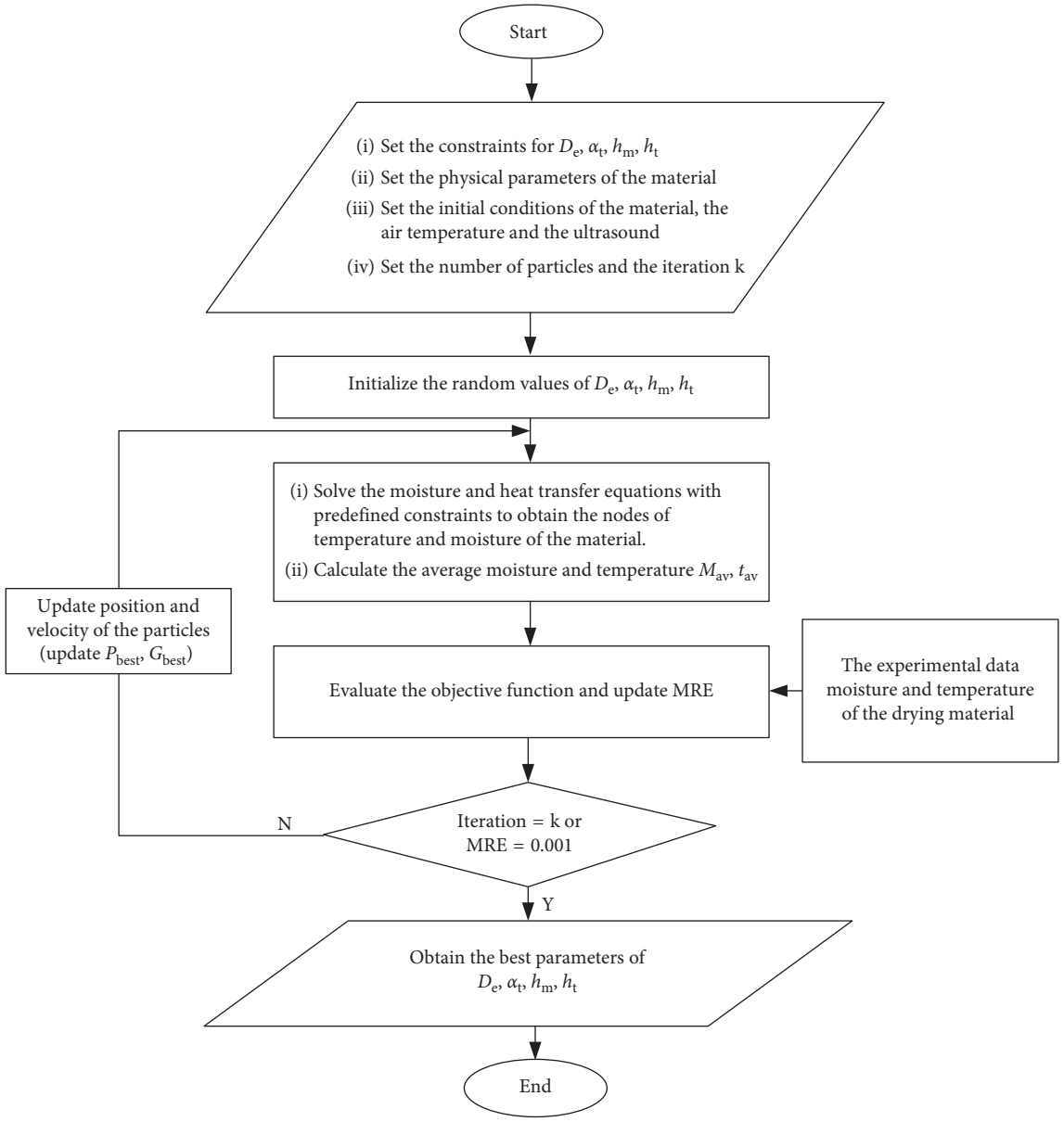


Figure 2: Flowchart for determining the values of D_e, α_t, h_m, and h_t.

The objective equations (16) and (17) are defined as

$$\mathrm{MRE}_i = \alpha \mathrm{MRE}_{M,i} + (1-\alpha)\mathrm{MRE}_{t,i}, \tag{16}$$

$$\mathrm{Min}\{\mathrm{MRE}_i\}, \tag{17}$$

where MRE (mean relative percentage error) is the relative difference between the values of calculations and experimental data. The $\mathrm{MRE}_{M,i}$ is MRE of moisture content, $\mathrm{MRE}_{t,i}$ is MRE of temperature, and α is a weight (0-1), in this study, $\alpha = 0.5$.

A calculation program based on the PSO algorithm and other programs were performed by MATLAB 2015.

2.8. Color Change of the Drying Products. The product color is the quality evaluation criteria for dried ginseng roots [22], the CIE Lab color parameters (L^*, a^*, and b^*) were adopted to describe color change during our drying process. The values of L^*, a^*, and b^* were measured by the color measurement machine from X-Rite Inc. Grand Rapids MI (RM200). The data validity was confirmed by taking the average of three repeated measurements. The color change index (ΔE) was calculated by using the color parameters of the dried product as described by the following equation [23]:

$$\Delta E = \sqrt{\left(L^* - L^*_{\mathrm{ref}}\right)^2 + \left(a^* - a^*_{\mathrm{ref}}\right)^2 + \left(b^* - b^*_{\mathrm{ref}}\right)^2}, \tag{18}$$

where L^*_{ref}, a^*_{ref}, and b^*_{ref} are the standard values and in this study were values of the fresh material (before drying).

2.9. Statistical Analysis. To evaluate the fitness of the mathematical model, these following equations (19)–(21)

including, R^2 (coefficient of determination), RMSE (root mean square error), and MRE (mean relative percentage error) were considered [19]:

$$R^2 = 1 - \frac{\sum_{i=1}^{N}\left(y_{\exp,i} - y_{\mathrm{pre},i}\right)^2}{\sum_{i=1}^{N}\left(y_{\exp,i} - y_{\mathrm{av}}\right)^2}, \quad (19)$$

$$\mathrm{RMSE} = \sqrt{\frac{1}{N}\sum_{i=1}^{N}\left(y_{\exp,i} - y_{\mathrm{pre},i}\right)^2}, \quad (20)$$

$$\mathrm{MRE} = \frac{100\sum_{i=1}^{N}\left(\left|y_{\exp,i} - y_{\mathrm{pre},i}\right|\right)/y_{\exp,i}}{N}, \quad (21)$$

where $y_{\exp,i}$, $y_{\mathrm{pre},i}$, y_{av}, and N are the measured data from the experiment, the predicted values, the average experimental values, and the number of experiments, respectively.

Experiments were conducted in triplicate. All values were obtained in the average ± standard deviation ($n = 3$).

Regression analysis was performed by statistical software SAS 9.1.

3. Results and Discussion

3.1. The Ultrasonic Absorption Coefficient of C. javanica. Figure 3 shows the average temperature of *C. javanica* with and without ultrasound. The temperature difference at the point A (Δt_A), point B (Δt_B), and the average temperature difference of the material (Δt_{av}) with and without ultrasound are the average values of three repetitions. The standard errors in Figure 3 are relatively small, indicating good repeatability of experiments. The experimental results are illustrated in Table 1.

Figure 3 shows that the temperature inside the drying material when using ultrasound was higher than the temperature without ultrasound. The increased temperatures at the alternate positions of the drying material are different. The increased temperature (Δt) in the presence of ultrasound, calculated by equation (9), is the average value measured at points A and B. Here, the ultrasound intensity is in the range of 1.3–2.2 kW/m^2, and the values of Δt are higher without ultrasound, which are from 0.6 to 1.5°C. Linear regression analysis was performed by using the software SAS 9.1 with the data from Table 1, giving an ultrasonic absorption coefficient (μ_u) of *C. javanica* of 119.2 ($R^2 = 0.98$).

3.2. The Equilibrium Moisture Content of C. javanica. From the experimental data at three levels of temperature 30°C, 40°C, and 50°C, the nonlinear regression analysis determined the relationship between the equilibrium moisture content of *C. javanica*, the temperature, and water activity. Among the four chosen mathematical models, the modified Chung–Pfost model showed the worst indices: the least coefficient of determination ($R^2 = 0.95$), the largest values of RMSE (=0.13), and MRE (=14.71%). In contrast, the Oswin model gave the best values of $R^2 = 0.99$, RMSE = 0.001, and MRE = 1.22%. The experimental data and predictions from the Oswin model (equation (22)) are shown in Figure 4:

$$M_e = (0.120438 - 0.0005t)\left[\frac{a_w}{1 - a_w}\right]^{(0.4+0.001958t)}. \quad (22)$$

Equation (22) was chosen to calculate the water activity of *C. javanica* and was applied at the boundary conditions (equation (6)) when solving the equations (1) and (2) of heat and moisture transfer.

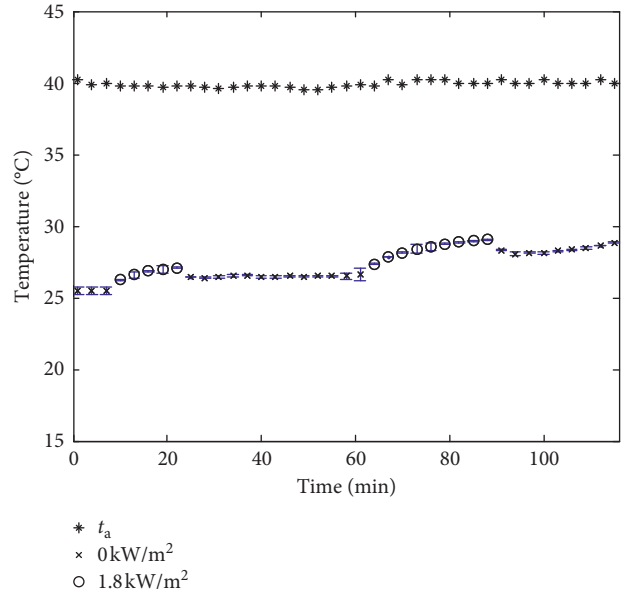


Figure 3: The average temperature (average ± SD, $n = 3$) of the drying material at the conditions: $t_a = 40$°C; $v_a = 0.5$ m/s; $\varphi_a = 22$–23%; ultrasonic intensity $I_u = 1.8$ kW/m^2.

Table 1: The difference temperatures (average ± SD, $n = 3$) with and without ultrasound for 5 minutes.

Cases	Ultrasound intensity (kW/m^2)	Difference temperature (°C)		
		Δt_A	Δt_B	Δt_{av}
1	1.3	0.8 ± 0.014	0.4 ± 0.014	0.6 ± 0.030
2	1.8	1.4 ± 0.066	0.9 ± 0.008	1.2 ± 0.022
3	2.2	1.9 ± 0.113	1.1 ± 0.084	1.5 ± 0.080

3.3. Drying Kinetics of C. javanica

3.3.1. Experimental Drying Data. Experiments were carried out at three levels of temperature, with and without ultrasound at three different values of intensity. The weight and temperature at points A and B are updated and stored on a computer with respect to drying time. The moisture content of *C. javanica* was calculated using equation (7). The average temperature at a certain time is the average temperature measured at points A and B at that time. The drying curve (moisture of the drying material) and temperature inside the sample of 12 different experiments along with the standard error bars are illustrated in Figures 5–7 and show that the

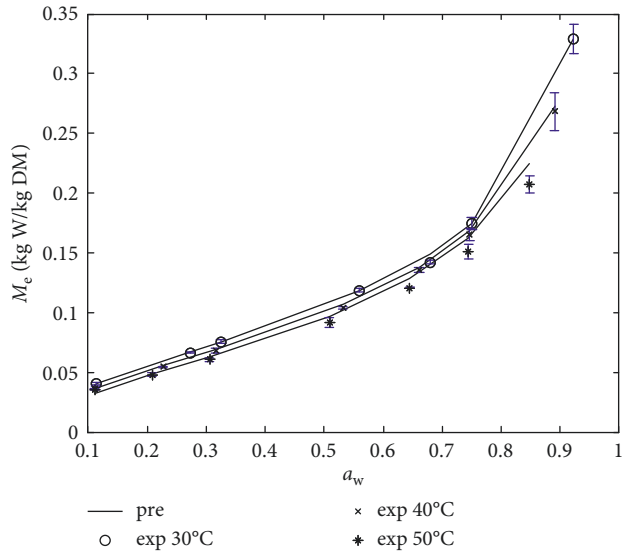


FIGURE 4: Experimental (exp) (average ± SD, $n = 3$) and predicted (pre) moisture content of *C. javanica* at 30°C, 40°C, and 50°C.

experiment had good repeatability as indicated by the low values of the standard error.

To prove the effectiveness of the ultrasound during the drying process, the drying time to reduce the moisture ($\Delta\tau$) of *C. javanica* from 7.0 to 0.44 (kg W/kg DM) and the increased temperature for the first 30 minutes (Δt), with and without ultrasound are considered. The experimental data are shown in Table 2.

The experimental data show that with the support of ultrasound, the drying time decreases, especially at the higher ultrasound intensity. When air temperature was 45°C, and the highest intensity was used (2.2 kW/m^2), the drying time reduces up to 45% compared with no ultrasound. However, higher air temperature is less effective with ultrasound on the drying time, such as at 50°C, the drying time is reduced to 28% at the highest intensity compared with without ultrasound use.

In addition, based on the experimental data, we concluded that when using ultrasound, the temperature in the drying material increased faster. Considering the air temperature at 40°C, in the first 30 minutes, the temperature in the drying material increased by 0.7°C without ultrasound and by 1.4°C, 1.6°C, and 2.8°C with ultrasound at intensities of 1.3 kW/m^2, 1.8 kW/m^2, and 2.2 kW/m^2, respectively. Moreover, part of the energy was absorbed and converted into thermal energy, making the temperature in the drying material greater than the temperature of the air, 0.6–2.1°C.

3.3.2. Parameters of Drying Kinetics. Based on the theoretical calculations, the experimental data, and the PSO algorithm, the four parameters (D_e, a_t, h_m, and h_t) related to the drying kinetics of *C. javanica* were obtained. Figure 8 shows a typical result of the average moisture content and the average temperature of the drying material at the air temperature of 45°C and intensity of 1.8 kW/m^2. The results of 12 cases including moisture and thermal diffusivity, convective heat, and moisture transfer coefficient at the surface of the material and the value of the objective function (MRE index) are shown in Table 3.

Table 3 shows that the average differences (MRE) between the calculations of equations (12) and (13) and the experiments are from 2.2% to 6.8%. Therefore, the parameters of the drying kinetics can be accepted as stated in the literature [19] (the MRE value must be less than 10%).

(1) The Effects of the Ultrasound on the Effective Moisture Diffusivity and Convective Moisture Transfer at the Surface of the Material. Table 3 shows that D_e and h_m values depend on the air temperature and the intensity of ultrasound; higher values of temperature and intensity results in higher values of D_e and h_m. In the air temperature range 40–50°C and the ultrasound intensity of 0 to 2.2 kW/m^2 (0–100 W), the D_e and h_m values are from 3.2×10^{-10} to 6.7×10^{-10} m^2/s and 2.3×10^{-3} to 4.1×10^{-3} kg/m^{2}s, respectively. The values of D_e, in this study, are in the range of the effective moisture diffusivity of food, between 10^{-11} and 10^{-9} m^2/s as stated in [11]. Also, similar to previously stated orange peel [6] values, D_e is between 0.88×10^{-9} and 1.72×10^{-9} m^2/s, and h_m is between 1.17×10^{-3} and 2.43×10^{-3} kg/m^{2}s at an air temperature and moisture of 40°C and 26.5%, respectively, the power of the ultrasound was in the range 0–90 W. Other like examples include, values of D_e between 0.14×10^{-10} and 0.74×10^{-10} m^2/s for salted codfish [7] and between 0.763×10^{-10} and 2.293×10^{-10} m^2/s for strawberries [11]. The values of h_m for strawberries are also between 1.380×10^{-5} and 3.387×10^{-5} kg/m^{2}s at the air temperature of 40–70°C and with an ultrasound power between 0 and 60 W [11].

In this study, with use of ultrasound, the increase in D_e is inversely proportional to the air temperature (25–75% at 40°C, 26–64% at 45°C, and 18–28% at 50°C). This is similar to h_m (22–56% at 40°C, 12–37% at 45°C, and 11–26% at 50°C). Therefore, we concluded that the ultrasound has a profound effect on the effective moisture diffusivity in the drying material and convective moisture transfer at surface of the material at lower air temperature. These effects decrease as the air temperature increases.

A nonlinear model was proposed by Rodríguez et al. [4] as in equations (23) and (24) for effective moisture diffusivity and external mass transfer coefficients, respectively:

$$D_e = d_1 e^{\left(-\left(d_2/\left(273.15+t_a\right)\right)-d_3P-\left(d_4P/\left(273.15+t_a\right)^2\right)+d_5/\left(273.15+t_a\right)\right)}, \tag{23}$$

$$h_m = h_1 - \frac{h_2}{\left(273.15 + t_a\right)} - h_3P - \frac{h_4P}{\left(273.15 + t_a\right)^2} + \frac{h_5}{\left(273.15 + t_a\right)}. \tag{24}$$

In this study, a nonlinear model was developed based on equations (23) and (24) and nonlinear regression analysis in the form of a second-order function. The relationships between the identified parameters (D_e, h_m, the air temperature, and the ultrasound intensity) are shown in Figure 9 and in the following equations:

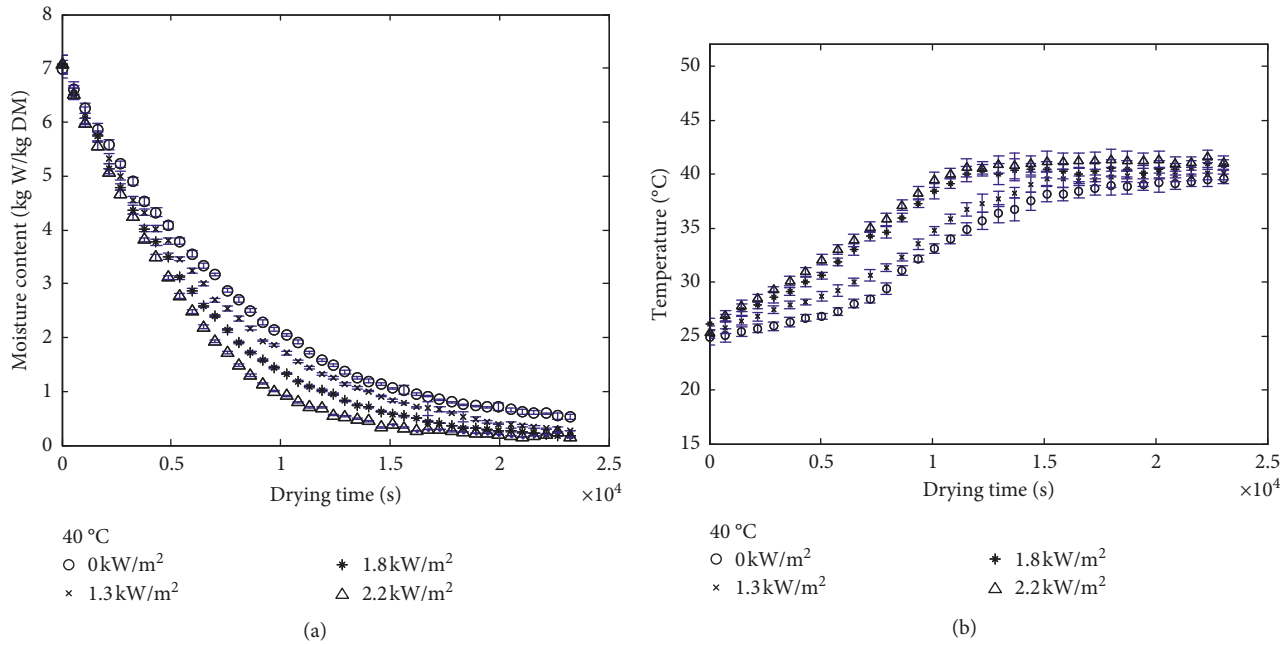


Figure 5: Drying kinetics at drying air parameters: 40°C, 0.5 m/s, and 20–23% air relative humidity. (a) Drying curves; (b) increasing temperatures (average ± SD, $n = 3$).

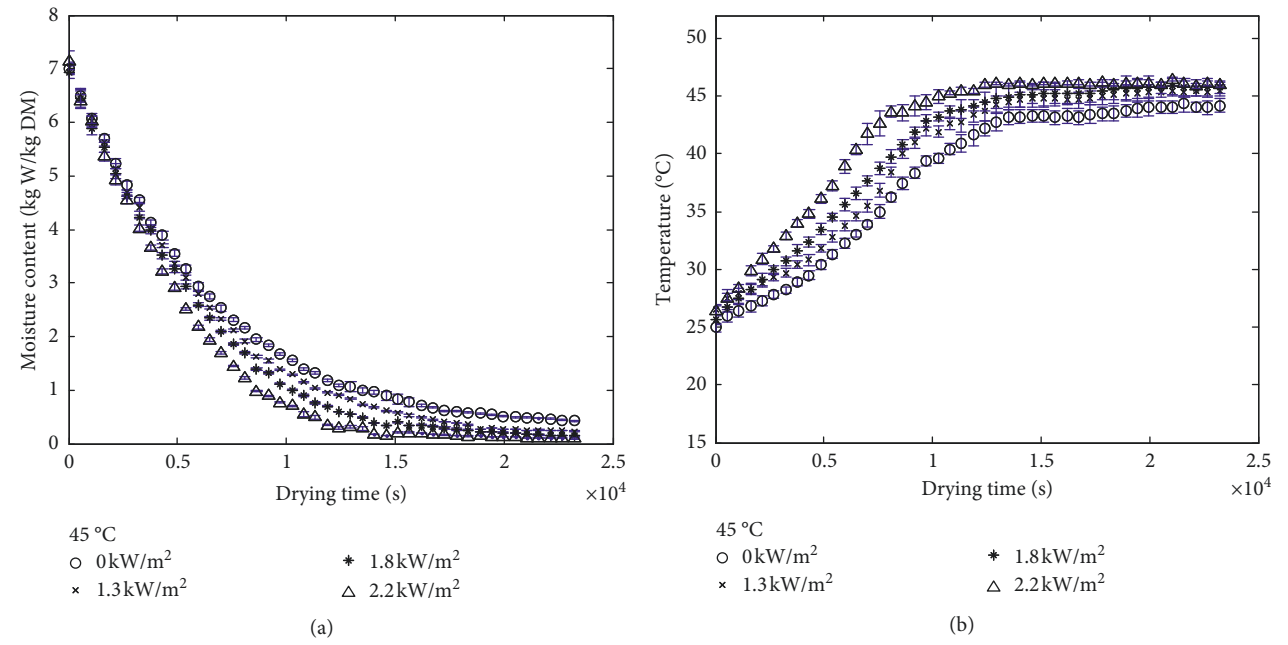


Figure 6: Drying kinetics at drying air parameters: 45°C, 0.5 m/s, and 18–20% air relative humidity. (a) Drying curves; (b) increasing temperatures (average ± SD, $n = 3$).

$$D_e = 3.05 \times 10^{-4} e^{\left(-\left(4286.96/\left(273.15+t_a\right)\right)+2.202967I_u-\left(212275I_u/\left(273.15+t_a\right)^2\right)+24418.8I_u^2/\left(273.15+t_a\right)-\left(3710120I_u^2/\left(273.15+t_a\right)^2\right)-40.04I_u^2\right)}, \quad (25)$$

where $R^2 = 0.99$, RMSE = 0.010, and MRE = 0.96%.

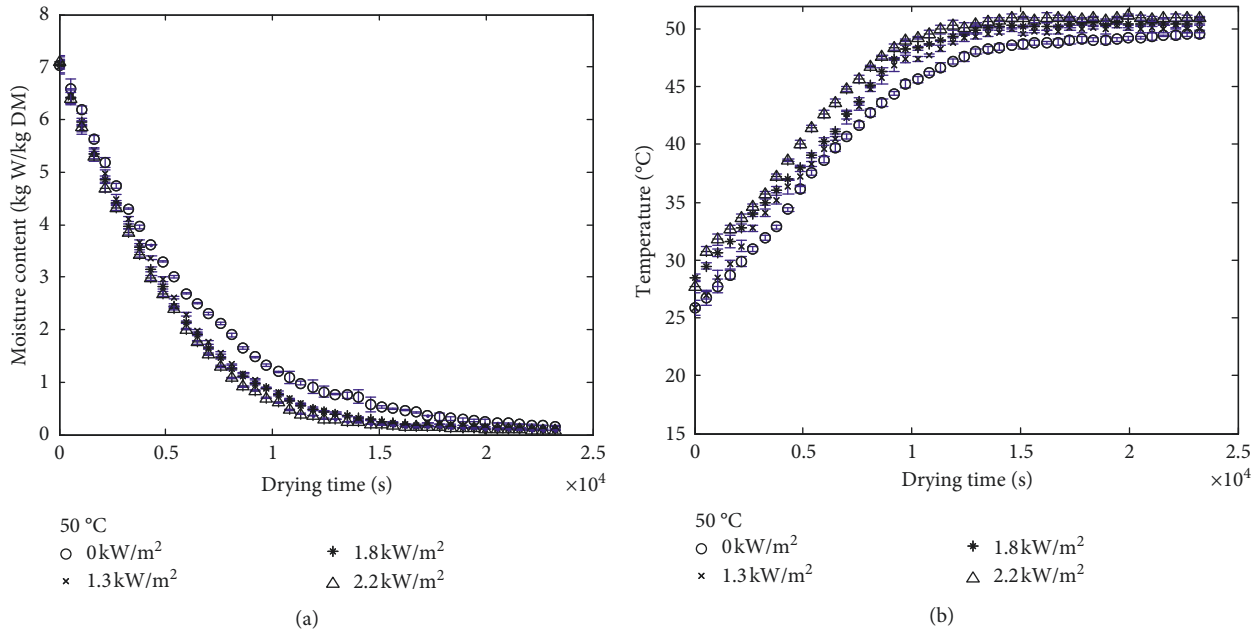


Figure 7: Drying kinetics at drying air parameters: 50°C, 0.5 m/s, and 15–17% air relative humidity. (a) Drying curves; (b) increasing temperatures (average ± SD, $n = 3$).

Table 2: The drying time of *Codonopsis javanica* with and without the ultrasound.

Cases	Ultrasound intensity, I_u (kW/m^2)	Air temperature, t_a (°C)	Drying time, τ (s)	The reduced drying time, $\Delta\tau$ (%)
1	0	40	23900	—
2	1.3		19000	20
3	1.7		16700	30
4	2.2		14000	41
5	0	45	21900	—
6	1.3		16500	25
7	1.8		13800	37
8	2.2		12100	45
9	0	50	16700	—
10	1.3		12900	23
11	1.8		12600	24
12	2.2		12000	28

Table 3: Parameters (D_e, a_t, h_m, and h_t) of *Codonopsis javanica* at different conditions.

Cases	I_u (kW/m^2)	t_a (°C)	$D_e \times 10^{-10}$ (m^2/s)	$\alpha_t \times 10^{-7}$ (m^2/s)	$h_m \times 10^{-3}$ (kg/m^{2}s)	h_t (W/m^{2}K)	MRE (%)
1	0	40	3.2	1.01	2.3	29.2	3.3
2	1.3		4	1.13	2.8	39.8	3.1
3	1.8		4.6	1.27	3.2	48.8	3.4
4	2.2		5.6	1.32	3.8	60.1	6.8
5	0	45	3.9	1.16	2.9	30.7	3.0
6	1.3		4.9	1.30	3.2	40.7	2.7
7	1.8		5.7	1.35	3.6	51.2	2.9
8	2.2		6.4	1.37	4.0	62.4	4.4
9	0	50	4.9	1.27	3.4	33.2	2.7
10	1.3		5.9	1.35	3.6	41.6	2.2
11	1.8		6.4	1.37	3.9	53.6	5.2
12	2.2		6.7	1.38	4.1	63.6	2.6

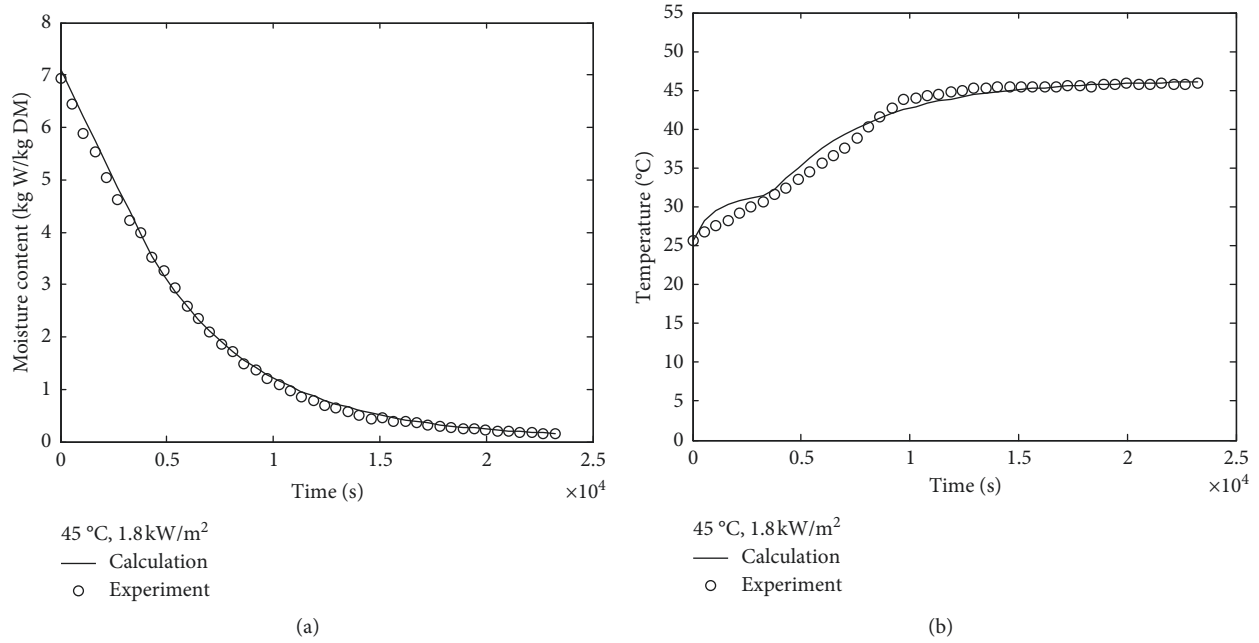


Figure 8: Calculation and experiment drying curves and temperature curves of *Codonopsis javanica* at 45°C air temperature and 1.8 kW/m^2 intensity: (a) change of moisture content; (b) temperature inside the sample.

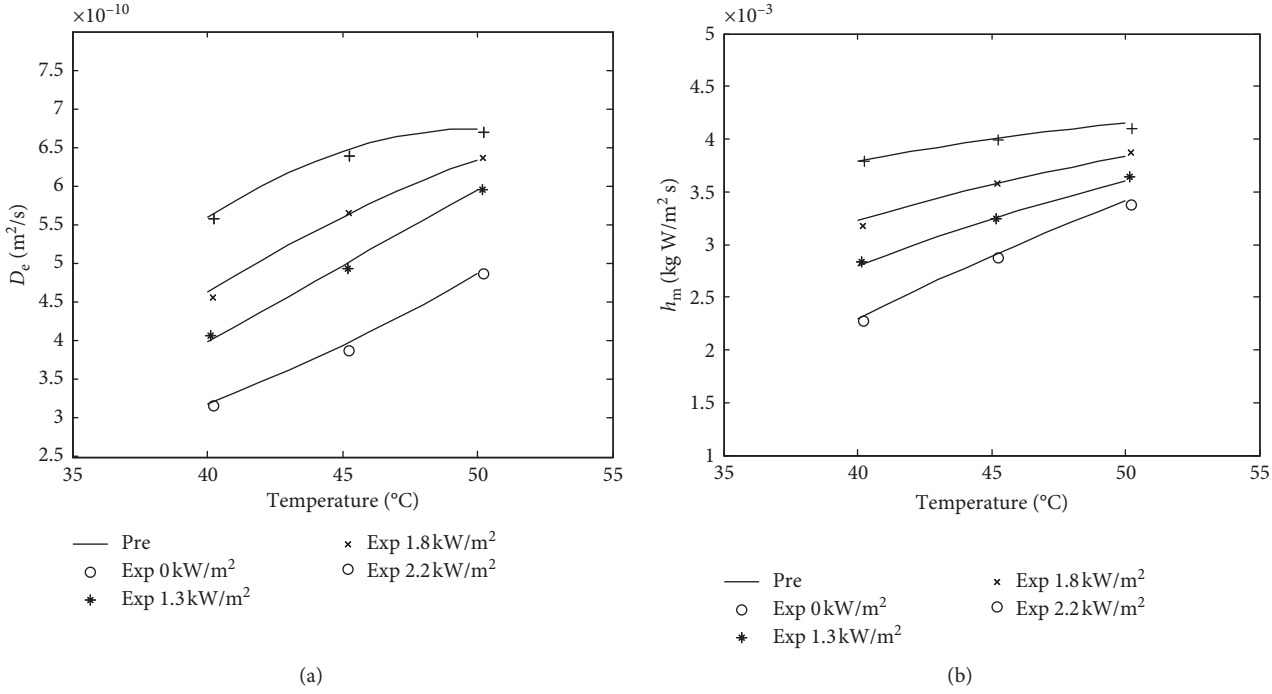


Figure 9: Influence of temperature on effective moisture diffusivity and convective moisture transfer coefficient at different ultrasound intensities: (a) the moisture diffusion coefficients and (b) the external moisture transfer coefficients of *Codonopsis javanica*.

$$h_m = 0.010032 - \frac{0.41659}{t_a} - 0.0031 I_u - \frac{5.3856 I_u}{t_a^2} + \frac{0.256727 I_u}{t_a} + \frac{0.515849 I_u^2}{t_a^2} + \frac{4.285627}{t_a^2}, \quad (26)$$

where $R^2 = 0.99$, RMSE = 0.008, and MRE = 0.63%.

(2) The Effects of the Ultrasound on the Thermal Diffusivity (α_t) and Convective Heat Transfer Coefficients (h_t) at the Surface of the Drying Material. The ultrasound propagating through the air affects the temperature kinetics of the drying material via the parameters α_t and h_t. According to the experimental results shown in Table 3, the values of α_t and h_t are in the range of 1.01×10^{-7} and 1.38×10^{-7} m^2/s and 29.2

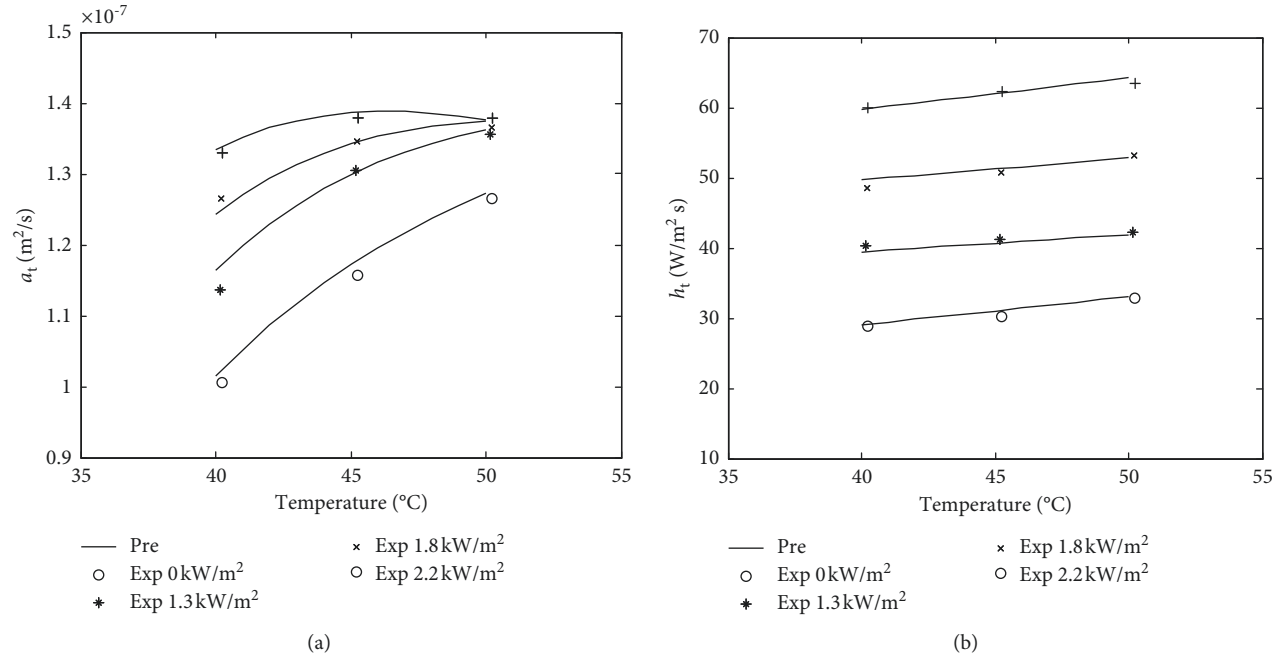


Figure 10: Influence of temperature on the thermal diffusivity and convective heat transfer coefficients: (a) the thermal diffusion coefficients and (b) the heat transfer coefficients of *Codonopsis javanica*.

Table 4: Color of the dried *Codonopsis javanica* (average ± SD, $n = 3$).

Cases	I_u (kW/m^2)	t_a (°C)	L^*	a^*	b^*	ΔE
Material			71.8 ± 2.26	2 ± 0.05	31.6 ± 1.31	
1	0	40	79.2 ± 1.08	2.7 ± 0.13	21.4 ± 0.69	12.6 ± 0.42
2	1.3		78.6 ± 1.07	3.3 ± 0.06	23.9 ± 0.57	10.4 ± 0.20
3	1.8		78.5 ± 1.42	3.4 ± 0.04	25.5 ± 0.39	9.2 ± 0.11
4	2.2		76.8 ± 1.12	4.2 ± 0.11	22.5 ± 0.36	10.6 ± 0.32
5	0	45	75.1 ± 1.46	5.8 ± 0.10	21.6 ± 0.50	11.2 ± 0.23
6	1.3		78.4 ± 1.31	4.5 ± 0.10	26.2 ± 0.43	8.8 ± 0.18
7	1.8		78.2 ± 6.66	5.4 ± 0.19	27.3 ± 2.45	8.4 ± 0.82
8	2.2		72.6 ± 1.93	5.9 ± 0.19	23.7 ± 1.31	8.8 ± 0.56
9	0	50	59.6 ± 1.74	6.1 ± 0.18	30.8 ± 0.74	12.9 ± 0.19
10	1.3		61.6 ± 0.97	6.1 ± 0.13	30.8 ± 0.75	11.0 ± 0.18
11	1.8		61.6 ± 1.13	6.8 ± 0.62	33.1 ± 0.76	11.4 ± 0.24
12	2.2		60.1 ± 2.2	7.1 ± 0.30	32.8 ± 0.96	12.8 ± 0.51

and 63.6 W/m^2 K, respectively. In another research with other drying materials, the h_t of salted codfish is between 21.0 and 27.5 W/m^2 K [14]; α_t and h_t of potato are 1.31×10^{-7} m^2/s and 25–250 W/m^2 K, respectively [24].

Based on Table 3 data, the relationships between α_t, h_t, the air temperature, and ultrasound intensity are illustrated in Figure 10 and in the following equations:

$$\alpha_t = 1.014 \times 10^{-7} + \frac{6.553 \times 10^{-6}}{t_a} - 6.53 \times 10^{-8} I_u - \frac{1.3 \times 10^{-4} I_u}{t_a^2} + \frac{6.242 \times 10^{-6} I_u}{t_a} + \frac{1.7 \times 10^{-5} I_u^2}{t_a^2} - \frac{2.6 \times 10^{-4}}{t_a^2} - 7.16 \times 10^{-9} I_u^2, \quad (27)$$

where $R^2 = 0.98$, RMSE = 0.013, and MRE = 0.97%.

$$h_t = 56.64 + 2.20 t_a - \frac{34.54}{I_u} + \frac{4 t_a}{I_u^2} - \frac{5.63 t_a}{I_u}; \quad \text{with } U$$
$$= 13.03 + 0.4 t_a; \quad \text{with NU}, \quad (28)$$

where, with ultrasound-assisted (with U), $R^2 = 0.99$, RMSE = 0.010, and MRE = 0.83%. Without ultrasound-assisted (with NU) $I_u = 0$ kW/m^2, $R^2 = 0.97$, RMSE = 0.020, and MRE = 0.91%.

3.4. Color Change of C. javanica. The color parameters of the products at the different drying conditions were measured and shown in Table 4.

Table 4 shows that when air temperature increases, the value of L^* (lightness) decreases, but the values of a^* (redness/greenness) and b^* (yellowness/blueness) increase

proportionally along with the ultrasound intensity. That is similar to the results reported by Wei et al. for American Ginseng [22]. The value of ΔE changes of *C. javanica* is between 11.2 and 12.9 without ultrasound and between 8.4 and 12.8 with ultrasound at the intensity of 1.3–2.2 kW/m^2. We concluded that the color of the dried samples changes slightly compared with the fresh samples when using the ultrasound-assisted drying process. This can be explained as using ultrasound makes drying times shorter, causing less influence on the color of the product.

4. Conclusions

The thermal diffusion and moisture diffusion coefficients of *C. javanica* at air temperature 40–50°C, with and without ultrasound at the intensity of 1.3–2.2 kW/m^2 were investigated in this study. The results show that the values of thermal and moisture diffusivity are in the range of $1.01–1.38 \times 10^{-7}$ m^2/s and $3.2–6.7 \times 10^{-10}$ m^2/s, respectively. The convective heat and moisture transfer coefficients at the surface of the drying material were between $2.3 \times 10^{-3}–4.1 \times 10^{-3}$ kg/m^2s and 29.2–63.6 W/m^2 K, respectively. In this study, the overall color differences considered the effectiveness of ultrasound as a way to preserve the quality of the product.

Data Availability

The data used to support the findings of this study are included within the article and are available from the corresponding author upon request.

Conflicts of Interest

The authors declare they have no conflicts of interest in this study.

Acknowledgments

The authors thank Nong Lam University Ho Chi Minh City and Ho Chi Minh City University of Technology and Education for supporting this study.

References

[1] G. Musielak, D. Mierzwa, and J. Kroehnke, "Food drying enhancement by ultrasound—a review," *Trends in Food Science & Technology*, vol. 56, pp. 126–141, 2016.

[2] P. Li and Z. Chen, "Experiment study on porous fiber drying enhancement with application of power ultrasoundfiber drying enhancement with application of power ultrasound," *Applied Acoustics*, vol. 127, pp. 169–174, 2017.

[3] R. M. S. C. Morais, A. M. M. B. Morais, I. Dammak et al., "Functional dehydrated foods for health preservation," *Journal of Food Quality*, vol. 2018, Article ID 1739636, 29 pages, 2018.

[4] Ó. Rodríguez, J. V. Santacatalina, S. Simal, J. V. Garcia-Perez, A. Femenia, and C. Rosselló, "Influence of power ultrasound application on drying kinetics of apple and its antioxidant and microstructural properties," *Journal of Food Engineering*, vol. 129, pp. 21–29, 2014.

[5] J. Crank, *The Mathematics of Diffusion*, Clarendon Press, Oxford, UK, 2nd edition, 1975.

[6] J. V. Garcia-Perez, C. Ortuño, A. Puig, J. A. Carcel, and I. Perez-Munuera, "Enhancement of water transport and microstructural changes induced by high-intensity ultrasound application on orange peel drying," *Food and Bioprocess Technology*, vol. 5, no. 6, pp. 2256–2265, 2012.

[7] C. Ozuna, J. A. Cárcel, P. M. Walde, and J. V. Garcia-Perez, "Low-temperature drying of salted cod (Gadus morhua) assisted by high power ultrasound: kinetics and physical properties," *Innovative Food Science & Emerging Technologies*, vol. 23, pp. 146–155, 2014.

[8] Y. Liu, Y. Sun, S. Miao, F. Li, and D. Luo, "Drying characteristics of ultrasound assisted hot air drying of Flos lonicerae," *Journal of Food Science and Technology*, vol. 52, no. 8, pp. 4955–4964, 2015.

[9] J. V. Santacatalina, O. Rodríguez, S. Simal, J. A. Cárcel, A. Mulet, and J. V. García-Pérez, "Ultrasonically enhanced low-temperature drying of apple: influence on drying kinetics and antioxidant potential," *Journal of Food Engineering*, vol. 138, pp. 35–44, 2014.

[10] C. Brines, A. Mulet, J. V. García-Pérez, E. Riera, and J. A. Cárcel, "Influence of the ultrasonic power applied on freeze drying kinetics," *Physics Procedia*, vol. 70, pp. 850–853, 2015.

[11] J. Gamboa-Santos, A. Montilla, J. A. Cárcel, M. Villamiel, and J. V. Garcia-Perez, "Air-borne ultrasound application in the convective drying of strawberry," *Journal of Food Engineering*, vol. 128, pp. 132–139, 2014.

[12] E. M. G. C. D. Nascimento, A. Mulet, J. L. R. Ascheri, C. W. P. D. Carvalho, and J. A. Carcel, "Effects of high-intensity ultrasound on drying kinetics and antioxidant properties of passion fruit peel," *Journal of Food Engineering*, vol. 170, pp. 108–118, 2016.

[13] J. Rodríguez, A. Mulet, and J. Bon, "Influence of high-intensity ultrasound on drying kinetics in fixed beds of high porosity," *Journal of Food Engineering*, vol. 127, pp. 93–102, 2014.

[14] M. Bantle and J. Hanssler, "Ultrasonic convective drying kinetics of clipfish during the initial drying period," *Drying Technology*, vol. 31, no. 11, pp. 1307–1316, 2013.

[15] M. Bantle and T. M. Eikevik, "A study of the energy efficiency of convective drying systems assisted by ultrasound in the production of clipfish," *Journal of Cleaner Production*, vol. 65, pp. 217–223, 2014.

[16] S. J. Kowalski and A. Pawłowski, "Intensification of apple drying due to ultrasound enhancement," *Journal of Food Engineering*, vol. 156, pp. 1–9, 2015.

[17] P. H. Tuan, N. V. T. Duong, and N. X. Quang, "Computational modeling and design of a high-intensity ultrasonic transducer with extensive radiator for food dehydration," in *Proceedings of the 2nd International Conference on Green Technology and Sustainable Development (GTSD2014)*, vol. 2, pp. 234–239, Ho Chi Minh City, Vietnam, October 2014.

[18] Y. J. Cho, S. J. Park, and C. H. Lee, "Latent heat of Korean ginseng," *Journal of Food Engineering*, vol. 30, no. 3-4, pp. 245–432, 1996.

[19] P. Yogendrarajah, S. Samapundo, F. Devlieghere, S. De Saeger, and B. De Meulenaer, "Moisture sorption isotherms and thermodynamic properties of whole black peppercorns (Piper nigrum L.)," *LWT—Food Science and Technology*, vol. 64, no. 1, pp. 177–188, 2015.

[20] X. Hu and R. Eberhart, "Solving constrained nonlinear optimization problems with particle swarm optimization," in

Proceedings of the Sixth World Multi Conference on Systemics, Cybernetics and Informatics, pp. 203–206, Orlando, FL, USA, July 2002.

[21] D. P. Rini, S. M. Shamsuddin, and S. S. Yuhaniz, "Particle swarm optimization: technique, system and challenges," *International Journal of Computer Applications*, vol. 14, no. 1, pp. 19–27, 2011.

[22] X. H. Wei, L. C. Lim, S. D. Wen, and G. Z. Jiang, "Color change kinetics of American ginseng (Panax quinquefolium) slices during air impingement drying," *Drying Technology*, vol. 32, no. 4, pp. 418–247, 2014.

[23] A. W. Deshmukh, M. N. Varma, C. K. Yoo, and K. L. Wasewar, "Investigation of solar drying of ginger (zingiberofficinale): empirical modelling, drying characteristics, and quality study," *Chinese Journal of Engineering*, vol. 2014, Article ID 305823, 7 pages, 2014.

[24] M. M. Hussain and I. Dincer, "Analysis of two-dimensional heat and moisture transfer during drying of spherical objects," *International Journal of Energy Research*, vol. 27, no. 21, pp. 703–713, 2003.